



LAWRENCE
LIVERMORE
NATIONAL
LABORATORY

Upper Wide-Angle Viewing System for ITER

C. J. Lasnier, A. G. McLean, A. Gattuso, R. O'Neill, M. Smiley, J. Vasquez, R. Feder, M. Smith, B. Stratton, D. Johnson, A. L. Verlaan, J. A. Heijmans

June 2, 2016

21st Topical Conference on High-Temperature Plasma
Diagnostics
Madison, WI, United States
June 6, 2016 through June 9, 2016

Disclaimer

This document was prepared as an account of work sponsored by an agency of the United States government. Neither the United States government nor Lawrence Livermore National Security, LLC, nor any of their employees makes any warranty, expressed or implied, or assumes any legal liability or responsibility for the accuracy, completeness, or usefulness of any information, apparatus, product, or process disclosed, or represents that its use would not infringe privately owned rights. Reference herein to any specific commercial product, process, or service by trade name, trademark, manufacturer, or otherwise does not necessarily constitute or imply its endorsement, recommendation, or favoring by the United States government or Lawrence Livermore National Security, LLC. The views and opinions of authors expressed herein do not necessarily state or reflect those of the United States government or Lawrence Livermore National Security, LLC, and shall not be used for advertising or product endorsement purposes.

Upper Wide-Angle Viewing System for ITER^{a)}

C. J. Lasnier,^{1,b)} A. G. McLean,¹ A. Gattuso,² R. O'Neil,² M. Smiley,² J. Vasquez,² R. Feder,³ M. Smith,³ B. Stratton,³ D. Johnson,³ A. L. Verlaan,⁴ and J.A.C. Heijmans⁴

¹Lawrence Livermore National Laboratory, P.O. Box 808, Livermore, CA 94551-0808, USA

²General Atomics, P.O. Box 85608, San Diego, CA 92186-5608, USA

³Princeton Plasma Physics Laboratory, Princeton, New Jersey 08543, USA

⁴TNO, P.O. Box 155, NL-2600 AD Delft, Netherlands

(Presented XXXXX; received XXXXX; accepted XXXXX; published online XXXXX)

The Upper Wide Angle Viewing System (UWAVS) will be installed on five upper ports of ITER. This paper shows major requirements, gives an overview of the preliminary design with reasons for some design choices, examines self-emitted IR light from UWAVS optics and its effect on accuracy, and shows calculations of signal-to-noise ratios for the two-color temperature output as a function of integration time and divertor temperature. Accurate temperature output requires correction for vacuum window absorption vs. wavelength and for self-emitted IR, which requires good measurement of the temperature of the optical components. The anticipated signal-to-noise ratio using presently available IR cameras is adequate for the required 500 Hz frame rate except at the lowest specified divertor temperature of 200 °C.

I. INTRODUCTION

The Upper Wide Angle Viewing System (UWAVS) is being provided for ITER by the U.S. This system will provide real-time, simultaneous visible (VIS) and infrared (IR) imaging of the ITER divertor region via optical systems located in five upper ports. It must provide temperature measurements for a wide area of the divertor (e.g., more than 65% of the outer target) for hot spot monitoring, plus visible and IR images for physics analysis. This system complements the Equatorial Wide Angle Viewing System, which primarily views the inner divertor target. The system must function reliably in the severe ITER environment. This includes neutrons and gamma rays, potential erosion of and deposition on first mirrors, mechanical shock and temperature excursions in the port plug, and electromagnetic forces. This paper presents an overview of the current design, ways that requirements are being met, and areas in need of further development. Many of the most important performance requirements, from Annex B of the Procurement Arrangement are given in Table I.

II. OVERVIEW OF THE DESIGN

Light passes from the tokamak through an 18 mm circular aperture, which helps protect the first mirrors from deposition and erosion. The shutter has a double-bellows actuated shutter with flexures instead of pivots. A radio-frequency (RF) discharge is planned to remove deposits from the first two mirrors, which have a single-crystal molybdenum surface and are proposed to have a Nilo 42 substrate to match the thermal expansion of the molybdenum. The port plug components are mounted in a Front End Optics Tube (FEOT), which consists of a bullnose module near the plasma and a cask made up of plates and fasteners (FIG. 1). The bullnose is designed to be replaceable using remote handling and contains the mirrors most likely to be damaged by plasma products (FIG. 2). The light is conveyed by mirrors

Table I. WAVS performance requirements

REQUIREMENT	VIS	IR
Spatial Coverage	65 % of the outer divertor target 60% of the outer baffle 15 % of the inner baffle 45 % of the dome area	
Wavelength Range	400-700 nm	3-5 μ m
Signal to Noise @ Target Temp:		
200 C	TBD	1
1000 C		1000
Transmission	3-7%	10%
Spectral Resolution	H-alpha, Be, C, Cu, Ne, Ar, Kr, W	2 colors (3.0-3.5 μ m and 4.5-5.0 μ m)
Spatial Resolution @ object plane 10.3 m	3mm	5mm
Temporal Resolution	1000 Hz	500 Hz
Windowing Mode	N/A	6% of full frame @ 50 kHz
Temperature Range	N/A	200-3600 C @ 500 Hz; 400-3600 C @ 50 kHz
Brightness Range	40 -1E5 cd / m2	N/A
Calibration Accuracy	30%	10%
Temperature Equivalent Resolution	N/A	20 C
Intensity Resolution	1%	N/A

through the port plug to the vacuum closure plate, where a double sapphire vacuum window is mounted. The two windows in series are required for safety of tritium containment.

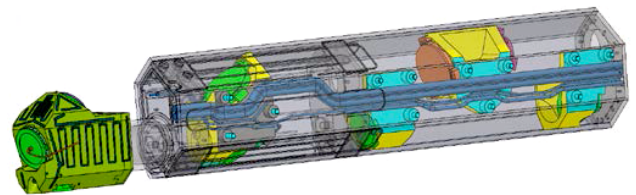


FIG 1. Front End Optics Tube including bullnose (left) and cask (right). Mirror groups are installed in blocks to preserve the most critical relative alignment.

^{a)} Contributed (or Invited) paper published as part of the Proceedings of the 21st Topical Conference on High-Temperature Plasma Diagnostics (HTPD 2016) in Madison, Wisconsin, USA.

^{b)} Author to whom correspondence should be addressed: Lasnier@llnl.gov.

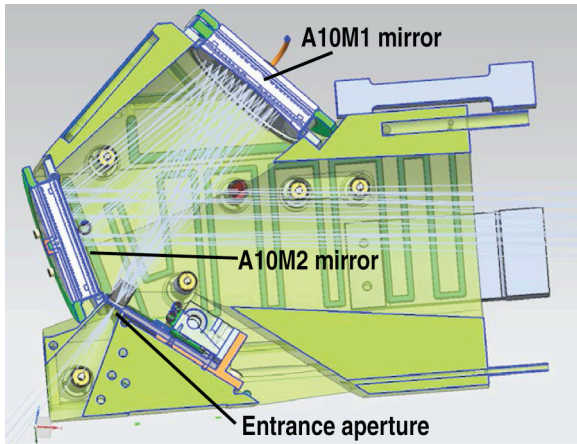


FIG 2. Bullnose view showing light path and first two mirrors, and entrance aperture.

Light exiting the vacuum window is carried by mirrors through the Port Interspace (FIG. 3), through the Bio-Shield wall (a thick concrete radiation shield), and into the Port Cell, where further relay, focusing, and splitting optics are located along with all the cameras.

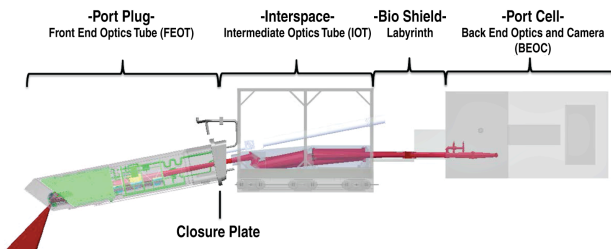


FIG 3. UWAVS system view, showing the light path through the FEOT, Port Interspace, Bio-Shield, and Back-End Optics

Each IR scene is viewed by two sets of cameras, with wavelengths of 3-3.5 μm and 4-4.5 μm to make up a two-color IR system. The longer wavelength band was changed from 4.5-5 microns to improve performance. The relative IR intensities of the two wavelengths are used to determine the temperature according to the slope of the Planck function.¹ This provides a temperature independent of the surface emissivity provided the emissivity is constant with wavelength. This is needed due to the tungsten divertor having low emissivity that most likely will change with time. Due to limited pixel numbers for existing IR camera detectors, the field of view is split between two cameras for each color, for a total of four IR cameras per UWAVS port. It is foreseen that future camera improvements may make this image split unnecessary. It is recommended that final camera purchase be delayed as long as feasible to allow IR camera technology development.

The use of mirrors in the FEOT and Interspace reduces the effect of radiation damage on the UWAVS system due to darkening of transmitting materials by neutron absorption. The mirrors also relay the visible and IR waves with the same ray path. The reflectivity of the metallic mirrors is higher in the IR than in the visible. The second two in-vacuum mirrors are to have a rhodium reflective surface layer. The remaining mirrors in the FEOT use a protected aluminum coating. The vacuum windows are to have a seven-layer anti-reflection coating for visible and IR light. The remaining mirrors serving both visible and IR light have a protected silver coating. The visible-IR beam splitters use CaF_2 substrates with multilayer and/or aluminum coatings. After

the visible-IR split, the IR mirrors use a gold coating to maximize IR throughput (37%-44% of the light at the aperture reaches the IR camera.). Visible-light mirrors use protected silver. The field of view for the visible light is not split between cameras as visible cameras today have a sufficiently high pixel count for the required spatial resolution.

Detailed seismic and vibration studies of the FEOT have been performed to prevent a mechanical resonance in the expected range of vibration frequencies for the port plug and to ensure it is strong enough to withstand anticipated forces due to earth motion. Electromagnetic and nuclear thermal loads have also been analyzed in detail. Electromagnetic loads principally affect the bullnose, its mirrors, and its connection to the cask, which are shown to meet the strength requirements. Nuclear heating also strongly affects the bullnose and progressively decreases along the FEOT; all mirrors require water cooling in order to maintain optical figure.

While not a consideration for most diagnostic optical systems in existing machines, heating of optical components in ITER UWAVS is a significant contributor to overall signal-to-noise ratio (SNR). Warm optics introduce IR radiation into the optical path that does not originate in the tokamak divertor or surrounding targets in the field of view. This spurious IR light adds extra IR intensity and distorts the shape of the IR spectrum because the optics have a different temperature than the divertor. FIG 4 shows the contributions of each of the optics in the FEOT and Interspace to the camera-measured intensity as a fraction of divertor IR intensity reaching the camera. The first four mirrors dominate the optics emission of IR except in the originally planned 4.5-5 μm band, where sapphire has increased absorption and therefore larger emission. This is the primary reason for

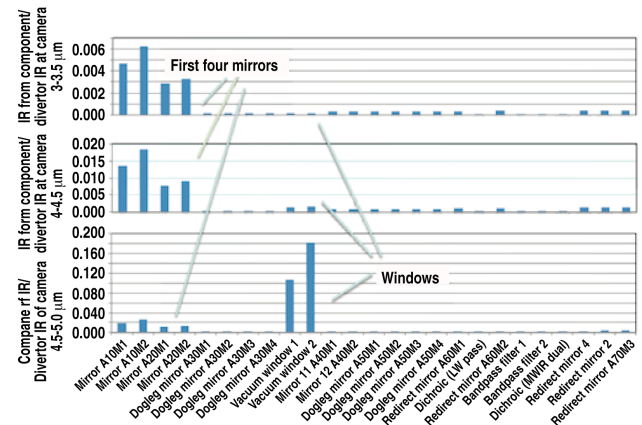


FIG 4. IR contributions by optics relative to divertor signal.

changing the longer wavelength band from 4.5-5.0 μm to 4.0-4.5 μm .

Simulations of the optical transmission of IR through the planned system and IR light emitted by optics and reaching the cameras have been performed. FIG. 5 shows two-color temperature fractional error as a function of the emissivity of the first mirror (called A10M1) for varying optics temperatures, at a divertor temperature of 200 $^{\circ}\text{C}$ (the lowest required divertor temperature to be measured by UWAVS and therefore the weakest IR signal). The allowed $\pm 10\%$ margin of error is exceeded in many cases, indicating that a correction must be made in the calculated two-color temperature.

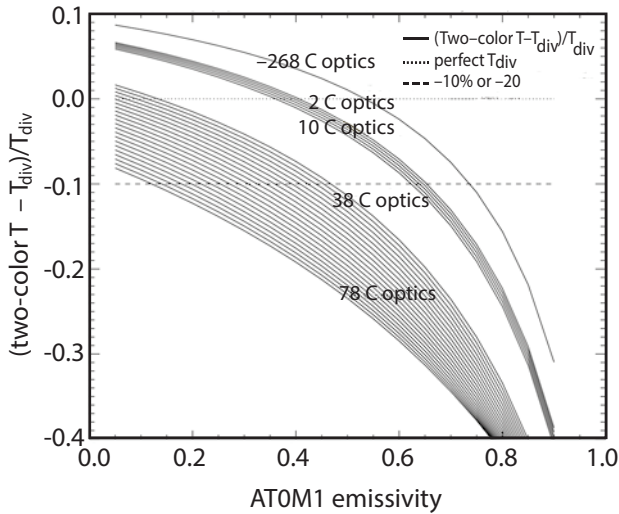


FIG 5. Two-color temperature fractional error vs. first-mirror emissivity for various optics temperatures, at a divertor temperature of 200 C.

In order to apply an accurate correction, the absorption vs. wavelength for the sapphire vacuum windows must be known, and the temperatures of the optics must be measured. In addition, the emissivities of the optics must be known with sufficient accuracy. Thermocouples with an accuracy of ± 2 °C are planned to measure the temperatures of the optics, although the first mirror temperature measurement scheme is not yet finalized due to a voltage isolation requirement for the RF discharge cleaning.

The different curves show the sensitivity of the temperature to errors in optics temperature measurements. All the optics were assumed to have the same temperature and the same temperature error, while in reality temperature measurement errors for the optics should be randomly distributed, producing some cancellation. The results shown in FIG. 5 represent an upper error bound.

The curves also show that the effect of optics temperature errors is magnified if mirror emissivity is not well known. Only the emissivity of the first mirror, which is expected to sustain the most damage, is treated here. It is reasonable to expect that the first mirror emissivity can be monitored to within $\pm 10\%$. The emissivities of the mirrors will be monitored using calibration filaments installed at locations in the optical train that send light to the cameras but do not block the view into the tokamak.

The SNR has been investigated for the two-color temperature by analyzing the IR emission for a given divertor temperature and the self-emitted IR from the optics, which produce a statistical photon shot noise. A typical IR detector noise and quantum efficiency were also assumed² to get the noise variation in the detected electron count for a camera measurement. A propagation of errors treatment was applied to the two single-color camera measurements, based on the temperature calculation equation in reference 1. The partial derivatives of that formula with respect to the each of the two single-camera intensities were used to determine the resulting noise level in the two-color output. Signal increases with integration time and noise increases as the square root of the photon count. FIG. 6 shows SNR for the two-color temperature

plotted vs. integration time for various divertor temperatures. For example, in order to exceed SNR=180 for a divertor temperature of 200 °C, an integration time of at least 6 ms is required. Measurements at 200 °C are most important for calibration during bake out where a longer integration time could be used to improve SNR. At 200 °C, the 500 Hz frame rate can still be achieved with the required SNR=1.

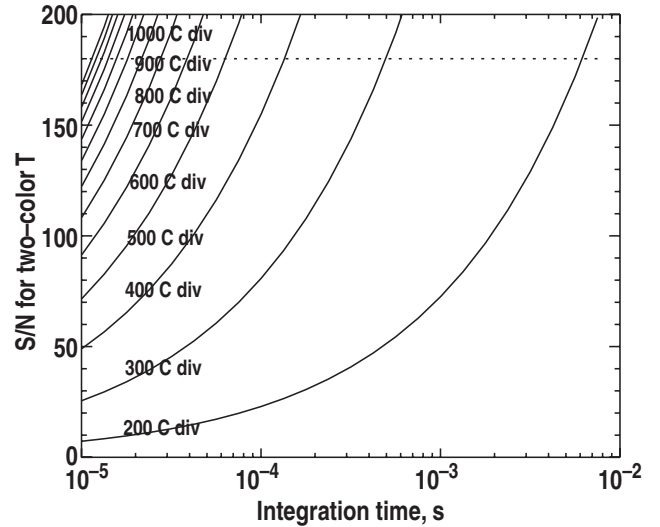


FIG 6. S/N for two-color temperature vs. integration time for various divertor temperatures, and optics at nominal operating temperature. The dotted line is SNR of 180.

The present state of the design provides a good compromise between optical throughput, protection of optics, good spatial and time resolution.

This work was performed in part under the auspices of the U.S. Department of Energy by Lawrence Livermore National Laboratory under Contract DE-AC52-07NA27344¹. This material is based upon work supported by the U.S. Department of Energy, Office of Science, Office of Fusion Energy Sciences.

¹ A.G. McLean, J.W. Ahn, R. Maingi, T.K. Grey, and A.L. Roquemore, "A dual-band adaptor for infrared imaging", Rev. Sci. Instrum. 83 (2012) 053706.

² S.D. Gunapala, S.V. Bandara, J.K. Liu, C.J. Hill, S.B. Rafol, J.M. Mumolo, J.T. Trinh, M.Z. Tidrow, and P.D. LeVan, "1024 × 1024 pixel

² S.D. Gunapala, S.V. Bandara, J.K. Liu, C.J. Hill, S.B. Rafol, J.M. Mumolo, J.T. Trinh, M.Z. Tidrow, and P.D. LeVan, "1024 × 1024 pixel mid-wavelength and long-wavelength infrared QWIP focal plane arrays for imaging applications", Semicond. Sci. Technol. 20 No. 5 (May 2005) 473.